RESEARCH ARTICLE

Editorial Process: Submission:03/10/2025 Acceptance:07/14/2025

Investigating *Andrographis paniculata* Compounds for Apoptosis Induction in Cancer

Quan Ke Thai[1]*, Phuoc Huynh[2], Tung Thanh Tran[3], Ba-Hai Nguyen[4], Huyen Thi Thuong Nguyen[5]

Abstract

Background: Reactivating the apoptosis pathway in cancer cells represents a crucial therapeutic strategy for cancer treatment, as malignant cells often evade apoptosis to sustain uncontrolled proliferation. Among the anti-apoptotic proteins, Bcl-xL has been implicated in the pathogenesis of various cancers due to its overexpression. Inhibition of this protein has therefore emerged as a key target for several FDA-approved anticancer drugs. In recent decades, research on natural compounds has increasingly shifted toward molecular-level understanding, facilitating the development of potent anticancer agents. One medicinal plant of interest is *Andrographis paniculata* (Burm.f.) Wall. ex Nees, which has shown a wide range of pharmacological activities, including potential anticancer properties. Methods: In this study, we curated a set of previously identified natural compounds from *A. paniculata* in LOTUS database that target Bcl-xL inhibition by in silico methods, included molecular docking and molecular dynamics simulation. **Results:** Our findings reveal three compounds exhibiting strong binding affinity toward the Bcl-xL protein. In silico analysis of their anticancer properties suggests that these compounds possess high potential as TP53 enhancers, anticarcinogenic, antineoplastic, apoptosis agonists, antimetastatic, cytostatic, antioxidant agents, and Myc inhibitors. Moreover, all three compounds conform to Lipinski's rule of five and show favorable drug-likeness characteristics. Molecular dynamics simulations over 100 ns, coupled with in-depth principal component analysis and binding free energy calculations, further support the stable and strong interactions of these compounds within the Bcl-xL active site. **Conclusions:** Natural compounds from *A. paniculata*, particularly andrographolide derivatives, exhibit stable and strong interactions with the Bcl-xL protein and possess multiple predicted anticancer activities. These findings support their potential as lead molecules for the development of Bcl-xL-targeted anticancer therapeutics.

Keywords: *Andrographis paniculata*- apoptosis- Bcl-xL protein- cancer- molecular dynamics

Asian Pac J Cancer Prev, **26 (7)**, 2657-2667

Introduction

Cancer remains the leading cause of mortality worldwide. According to GLOBOCAN statistics, in 2022, there were approximately 20 million new cancer cases and 9.7 million cancer-related deaths [1]. It is projected that the global incidence of cancer will rise to 35 million cases by 2050 [1]. The high mortality rate associated with cancer has underscored drug development as a central focus in the fight against this disease. Despite extensive efforts and the availability of multiple treatment modalities, including radiotherapy, chemotherapy, and surgical resection, their efficacy remains limited due to tumor heterogeneity, the emergence of drug-resistant cell populations, and complex tumor–microenvironment interactions [2-4]. Cancer development is a highly complex process involving multiple signaling pathways that regulate and control cellular function. One critical factor is the accumulation of unrepaired DNA mutations, leading to the expression of dysfunctional proteins that disrupt normal cellular physiology [5]. This results in the loss of cell cycle regulation, ultimately causing uncontrolled proliferation and tumor formation [6]. Apoptosis is a highly conserved mechanism of programmed cell death in eukaryotic organisms [7]. This process allows the elimination of defective cells in an orderly manner, thereby preventing unwanted inflammatory responses [7]. However, cancer cells can evade apoptosis, enabling their uncontrolled division and survival. Consequently, the induction of apoptosis in cancer cells has become a fundamental strategy and a key target in clinical cancer therapy [8].

Apoptosis is a highly regulated cellular process

*[1]Faculty of Natural science education, Saigon University, 273 An Duong Vuong, Cho Quan Ward, Ho Chi Minh City, Vietnam. [2]Graduate University of Science and Technology, Vietnam Academy of Science and Technology, Vietnam. [3]Vinh Phuc College, Phuc Yen City, Vinh Phuc Province, Vietnam. [4]Faculty of Pharmacy, Binh Duong Medical College, 529 Le Hong Phong, Phu Loi Ward, Ho Chi Minh City, Vietnam. [5]Department of Biology, HCMC University of Education, 280 An Duong Vuong Cho Quan Ward, Ho Chi Minh City, Vietnam. *For Correspondence: tkquan@sgu.edu.vn*

involving multiple signaling pathways. One of the key mechanisms governing apoptosis through the intrinsic mitochondrial pathway is controlled by the B cell lymphoma 2 (Bcl-2) protein family [9]. This family comprises approximately 20 members, categorized into two groups: anti-apoptotic proteins (e.g., Bcl-2, Bcl-w, A1, Mcl-1, Bcl-xL, …) and pro-apoptotic proteins (e.g., Bax, Bak, Bok, Bim, Bad, Bid, …) [10]. The balance between pro-apoptotic and anti-apoptotic members of the Bcl-2 family ultimately determines cell fate [11, 12]. Overexpression of anti-apoptotic members suppresses apoptosis by directly binding to pro-apoptotic proteins via a characteristic hydrophobic groove [13]. Specifically, Bcl-xL, an anti-apoptotic protein, can directly interact with Bax or Bak, preventing them from forming large membrane pores in the outer mitochondrial membrane. This inhibition blocks the release of cytochrome c from mitochondria, thereby halting the apoptotic cascade [13, 14]. The overexpression of Bcl-xL is strongly associated with cancer progression and tumor metastasis [15]. As a result, therapeutic agents targeting Bcl-xL are actively being developed to inhibit this protein and reactivate the apoptotic pathway [16, 17].

Conventional cancer treatments such as chemotherapy often lead to severe and undesirable side effects [18]. Consequently, the search for novel anticancer agents remains a critical and ongoing challenge for researchers. Natural compounds with pharmaceutical properties have garnered significant attention as alternatives to conventional chemotherapeutic agents due to their ability to target various cancer growth mechanisms, including cell proliferation, evasion of apoptosis, replicative immortality, invasion and metastasis, angiogenesis, and tumor-promoting inflammation [19]. Moreover, utilizing plant-derived natural compounds can reduce research timelines and lower the costs associated with cancer treatment. To date, numerous medicinal plants have demonstrated broad-spectrum anticancer properties [20-22]. Therefore, bioactive compounds derived from medicinal plants represent a valuable and effective resource for cancer therapy [20].

Andrographis paniculata (Burm. f.) Wall. ex Nees, a member of the Acanthaceae family, is a medicinal plant widely used in traditional medicine across Asia, the Americas, and Africa [23]. It is native to India and Sri Lanka and is commonly cultivated in various South and Southeast Asian countries, including China, Bangladesh, Cambodia, Indonesia, Laos, Malaysia, Myanmar, Thailand, Vietnam, and the Caribbean [24, 25]. *A. paniculata* has been recognized for its therapeutic potential in treating various conditions, including cancer, diabetes, high blood pressure, ulcers, leprosy, bronchitis, skin diseases, flatulence, colic, influenza, dysentery, dyspepsia, and malaria [23]. Furthermore, the World Health Organization has included *A. paniculata* in its monographs on widely used medicinal plants, highlighting its importance in quality control and herbal medicine applications [26]. Extensive research in Asia has identified that *A. paniculata* contains bioactive compounds such as labdane diterpenoid lactones and flavonoids, which exhibit broad-spectrum pharmacological properties [27, 28]. With advancements in bioinformatics tools and molecular biology, herbal medicine is increasingly recognized as a potential multi-target therapy due to the complex interactions between plant-derived compounds and various target proteins. Therefore, in this study, we systematically identified natural compounds from *A. paniculata* that exhibit strong binding affinity to the Bcl-xL protein, aiming to inhibit its function and subsequently trigger apoptosis, thereby preventing cancer cell survival.

Materials and Methods

Protein and Ligands preparation

The crystal structure of the Bcl-xL protein, resolved at a high resolution of 1.60 Å, was obtained from the Protein Data Bank (PDB ID: 6VWC) [29]. The Bcl-xL structure was prepared by the Maestro software (academic version). Hydrogen atoms were added, and partial charges were precisely calculated using the Gasteiger method in AutoDock Tools [30].

Natural compounds of *A. paniculata* were retrieved from the LOTUS database [31]. Data collection was conducted using in-house software developed in Python. Compounds from the LOTUS database that exhibited a Lipinski's rule of five failure value of 0 or 1 were retained for further analysis. In total, 193 eligible compounds from *A. paniculata* were collected. The 3D structures of these compounds were generated using Chem3D Pro version 12.0 (Cambridge Soft, USA) in the MM2 force field until they reached an energy-minimized state. Each molecular structure was further minimized using the MMFF94 force field, and up to 32 conformers were generated per compound by Open Babel software [32]. A total of 5,728 molecular structures were used for virtual screening.

Molecular docking

The ligand binding pocket on Bcl-xL was identified, providing the foundation for establishing our docking system to screen new compounds within this site. Docking simulations were performed using AutoDock GPU [33]. The docking grid was centered at coordinates x = 1.768, y = -1.392, and z = 11.868, with a grid box size of 70 × 70 × 70 and a spacing of 0.375 Å. Each ligand underwent 100 docking runs (n_run = 100), and the binding conformation with the lowest predicted free energy was recorded for each compound. The top three compounds with the highest binding affinity to Bcl-xL were selected for further analysis. The interactions between each ligand and Bcl-xL were subsequently analyzed using the Protein-Ligand Interaction Profiler (PLIP) server [34].

In silico pharmacokinetics and toxicological properties

The physicochemical and pharmacokinetic properties of the top compounds were assessed using the SwissADME server [35]. Toxicity profiles of the top hit compounds were predicted via the ProTox 3.0 server [36] and pkCSM server [37]. Anticancer activity predictions for the top compounds were conducted using the PASS server [38].

Molecular dynamics simulation

Classical molecular dynamics (MD) simulations of

the top hits were performed using GROMACS version 2023.5 [39]. Ligands were prepared using the CHARMM force field provided by the SwissParam server [40]. The simulation systems were parameterized based on the CHARMM36 force field [41]. Solvation was carried out using the TIP3P water model with 0.15 M NaCl concentration. The systems were relaxed through energy minimization until reaching an energy-stable state. Subsequently, each system underwent NVT and NPT equilibration for 100 ps at 300 K and 1 atm, employing the V-rescale thermostat with a time constant of 0.1 ps and the C-rescale barostat with a time constant of 2 ps. The production phase of the simulation was performed for 100 ns with a time step of 2 fs. Long-range electrostatic interactions were computed using the Particle Mesh Ewald method with a Coulomb cutoff of 1.2 nm, while short-range van der Waals interactions were truncated at 1.2 nm. The LINCS algorithm was applied to maintain holonomic constraints, and trajectory sampling was conducted every 10 ps. Post-simulation analysis was performed using built-in GROMACS utilities. Principal component analysis (PCA) was carried out to examine the convergence of ligand movements within each system using the MDTraj software package [42].

Binding free energy calculation

The free energy estimation of ligand binding to the Bcl-xL protein was performed using gmx_MMPBSA software [43]. The MM/GBSA algorithm was applied with default parameters, where the MM/GBSA equation was calculated as follows:

$$\Delta G_{MM/GBSA} = \Delta G_{Complex} - \Delta G_{Protein} - \Delta G_{ligand}$$

Each component of the total free energy was calculated using the following formula:

$$\Delta G = \Delta G_{vdW} + \Delta G_{Eletrostatic} + \Delta G_{GB} + \Delta G_{Non-polar}$$

where $\Delta G_{Eletrostatic}$, and ΔG_{vdW} represent electrostatic and Van der Waals interactions energies between protein and ligand, respectively, while ΔG_{GB} and $\Delta G_{(Non\text{-}polar)}$ account for the polar and non-polar solvation free energy contributions. The decomposition of free energy per residue between the protein and ligand was performed to identify key interacting amino acids.

Results

Molecular docking

The docking results revealed that three compounds of *A. paniculata*, LTS0160672, LTS0039075, and LTS0214223, exhibit high binding affinities to the Bcl-xL protein, with binding energies recorded at -17.00 (Kcal/mol), -16.89 (Kcal/mol), and -16.69 (Kcal/mol), respectively (Table 1). The compound LTS0160672 belongs to the diterpenoids chemical class, while both LTS0039075 and LTS0214223 are classified as flavonoids chemical class (Table 1). Docking analysis showed that all three compounds precisely bind within the hydrophobic pocket of the Bcl-xL protein (Figure 1). The interacting amino acids were also identified, with all three compounds forming hydrophobic interactions and hydrogen bonds with key amino acids of Bcl-xL, including 102ARG, 105PHE, 106SER, 108LEU, 130LEU, 139ARG, 146PHE, and 142ALA (Figure 1) (Table 2). These amino acids are crucial for the inhibition of pro-apoptotic proteins [44] and are key targets for interactions with other drugs [29]. Therefore, the stable interactions of the ligands within this hydrophobic pocket contribute to the inhibition of Bcl-xL protein activity.

Upon further investigation of other compounds, we observed that several other compounds from *A. paniculata* exhibit binding affinities almost identical to those of LTS0039075 and LTS0214223 (Figure 2). A common feature among these compounds is that they belong to the flavonoid chemical class, specifically flavonoid glycosides. This group consists of three flavonoid rings linked to hexose sugar via an O-glycosidic bond (Figure 2). The difference between these flavonoid glycosides lies in the substitution of functional groups on the flavonoid tricyclic (Figure 2). Upon querying the LOTUS database, we found that these compounds are characteristic of *A. paniculata* and do not appear in any other plant species. Our survey revealed that these compounds belong to the andrographidine of *A. paniculata*. Therefore, we hypothesize that andrographidine may represent a promising chemical with strong binding affinity to the hydrophobic pocket of the Bcl-xL protein. The top three compounds (LTS0160672, LTS0039075, and LTS0214223) were selected for further analysis.

In silico pharmacokinetics and toxicological properties

Extraction from LOTUS molecular profiles identified

Table 1. Top Hit Compounds of *A. paniculata* Interact with Bcl-xL Protein

LOTUS ID	Pubchem ID	Free energy of binding	IUPAC Name	Chemical class	Organism source
LTS0160672	85261364	-17.00 (Kcal/mol)	[6-[[1,4a-dimethyl-6-methylidene-5-[2-(5-oxo-2H-furan-4-yl)ethyl]-3,4,5,7,8,8a-hexahydro-2H-naphthalen-1-yl]methoxy]-3,4,5-trihydroxyoxan-2-yl]methyl acetate	Diterpenoids	Andrographis paniculata Potamogeton natans
LTS0039075	13963764	-16.89 (Kcal/mol)	2-(4-hydroxy-2,3-dimethoxyphenyl)-7,8-dimethoxy-5-{[3,4,5-trihydroxy-6-(hydroxymethyl)oxan-2-yl]oxy}-4H-chromen-4-one	Flavonoids	Andrographis paniculata
LTS0214223	13963768	-16.69 (Kcal/mol)	2-(2,3-dimethoxyphenyl)-7,8-dimethoxy-5-{[3,4,5-trihydroxy-6-(hydroxymethyl)oxan-2-yl]oxy}-4H-chromen-4-one	Flavonoids	Andrographis paniculata

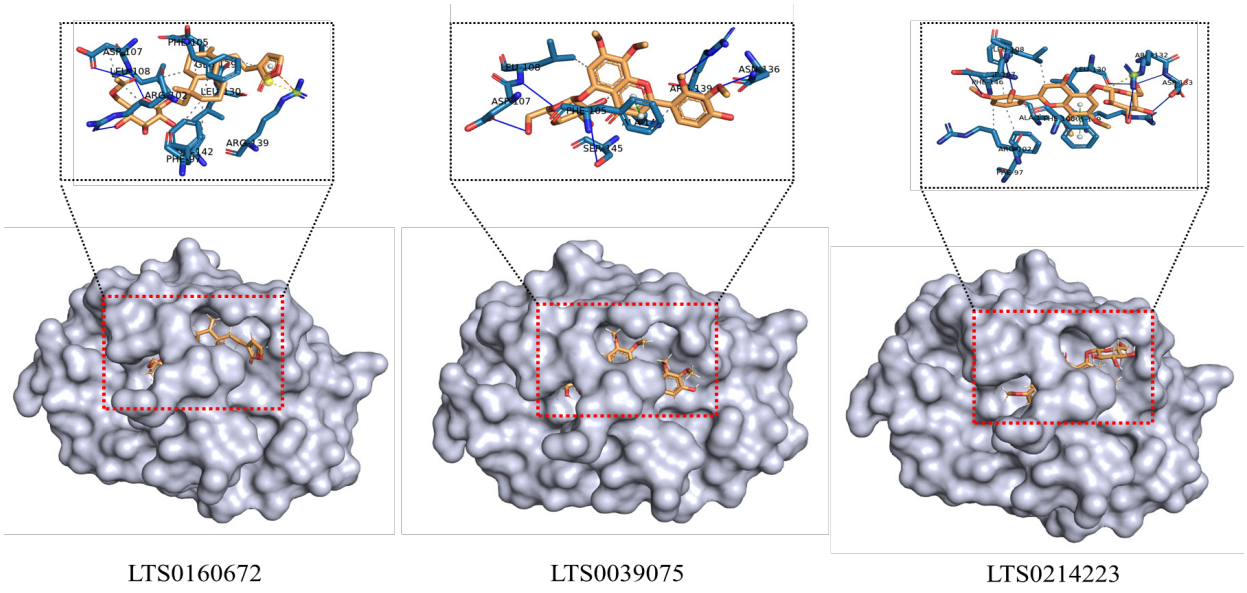

Figure 1. The Interaction of Top Hits in the Activity Pocket of Bcl-xL Protein

three compounds that violate only 1 Lipinski's rule of five, and ADME analysis indicates that these compounds are highly soluble in water, have good bioavailability, and do not cross the blood-brain barrier (Table 3). This suggests that these compounds are capable of entering cells and can potentially be developed as oral drugs. Toxicity profile analysis revealed that these compounds are not hepatotoxic, carcinogenic, mutagenic, and do not cause skin sensitization (Table 4). However, they may cause cardiac irritation, though the analysis was inconclusive as these compounds did not simultaneously inhibit both hERG I and hERG II receptors (Table 4). The use of *A. paniculata* extracts at the recommended dosage has shown safety and good tolerance, with no reported adverse effects

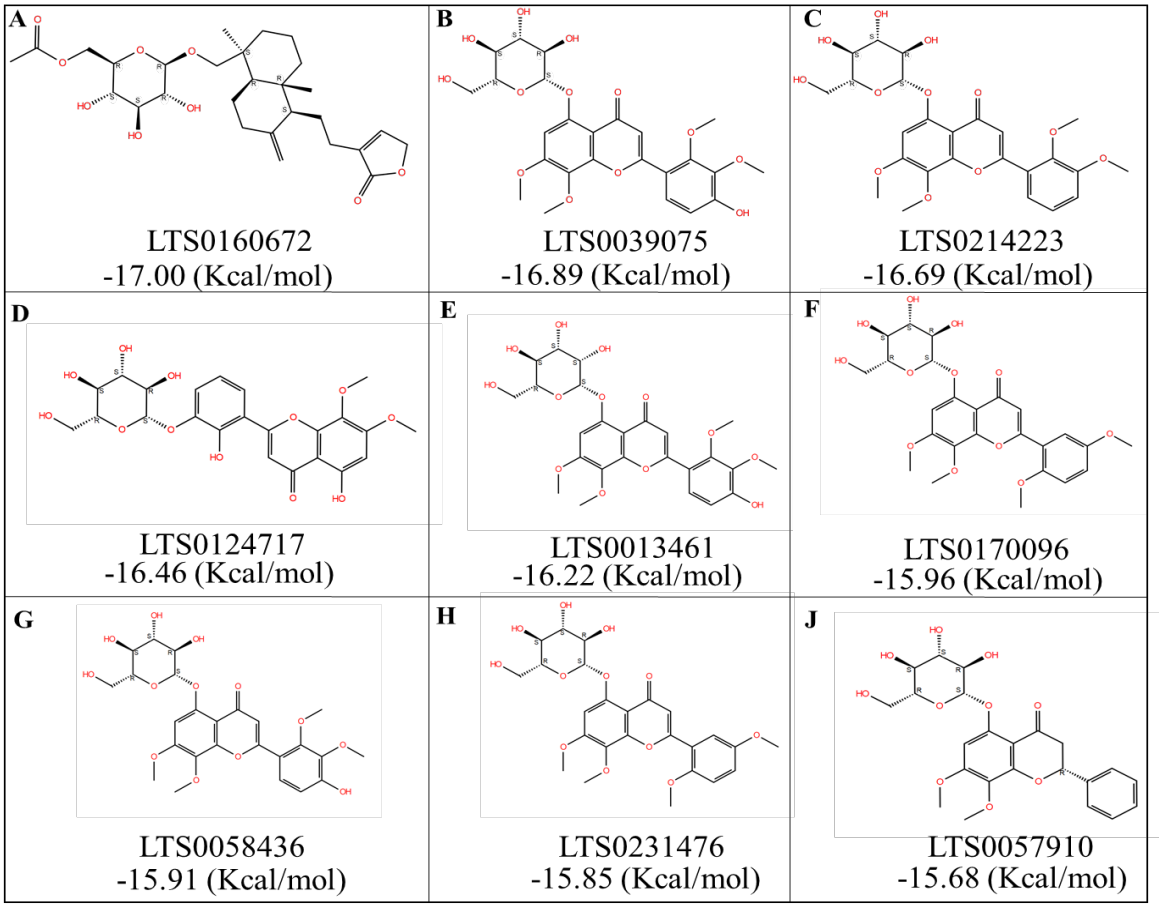

Figure 2. The Compounds of *A. paniculate* had High Affinity for Bcl-xL Protein

Table 2. Protein-Ligand Interaction Residues Profiles

Compounds	Hydrophobic interactions	Hydrogen bonds	π-Stacking	π-Cation	Salt Bridges
LTS0160672	97PHE, 102ARG, 105PHE, 107ASP, 108LEU, 129GLU, 130LEU, 142ALA	102ARG, 107ASP, 108LEU	-	139ARG	139ARG
	Total: 12	Total: 3		Total: 1	Total: 1
LTS0039075	105PHE, 108LEU, 139ARG, 142ALA	107ASP, 108LEU, 136ASN, 139ARG, 145SER	105PHE	-	-
	Total: 5	Total: 5	Total: 1		
LTS0214223	97PHE, 102ARG, 108LEU, 130LEU, 142ALA, 146PHE	107ASP, 108LEU, 132ARG, 133ASP, 134GLY, 139ARG	105PHE	-	132ARG
	Total: 6	Total: 7	Total: 1		Total: 1

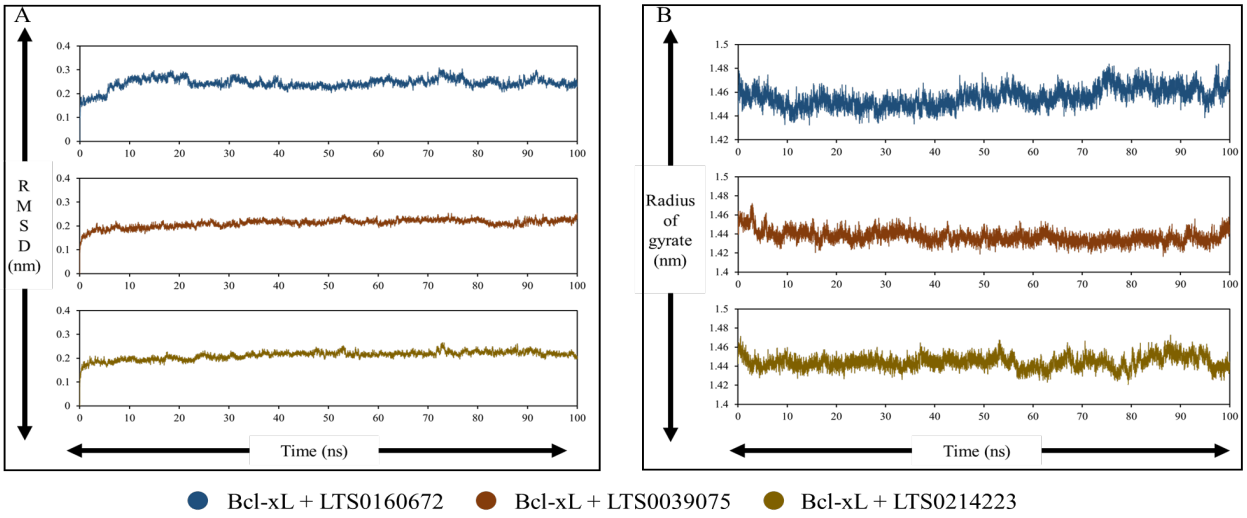

Figure 3. Root-Mean-Square Deviation and Radius of Gyration of Bcl-xL Protein in MD Simulations. (A. RMSD of Bcl-xL protein in complex with each top hit. B. Radius of gyration value of Bcl-xL in complex with different compounds. LTS0160672 (blue color); LTS0160672 (organge color); LTS0214223 (brown color)).

in many studies [45-48]. Except for LTS0160672, which is predicted to have a low LD50 of 9 mg/kg and belongs to Toxicity Class 2, the other two compounds have high tolerance levels and belong to Toxicity Class 5, which is considered relatively safe (Table 4). Analysis of oral rat LD50 values indicates acceptable average values for all three compounds (Table 4), and Tetrahymena pyriformis toxicity > -1 suggests that these compounds are safe

Table 3. Drug Likeness Property Analysis of Top Hits

	LTS0160672	LTS0039075	LTS0214223
Formula	$C_{28}H_{42}O_9$	$C_{25}H_{28}O_{13}$	$C_{25}H_{28}O_{12}$
Molecular weight	522.63 g/mol	536.48 g/mol	520.48 g/mol
Number of heavy atoms	37	38	37
Number of aromatic heavy atoms	0	16	16
Number of rotatable bonds	9	8	8
Number of H-bond acceptor	9	13	12
Number of H-bond donor	3	5	4
LogP	2.71	0.53	0.91
TPSA	131.75 Å²	186.74 Å²	166.51 Å²
Lipinski's rule of five failures	1	1	1
Water solubility	Soluble	Soluble	Soluble
GI absorption	High	Low	Low
BBB permeant	No	No	No
P-gp substrate	Yes	Yes	Yes
Bioavailability Score	0.55	0.17	0.17

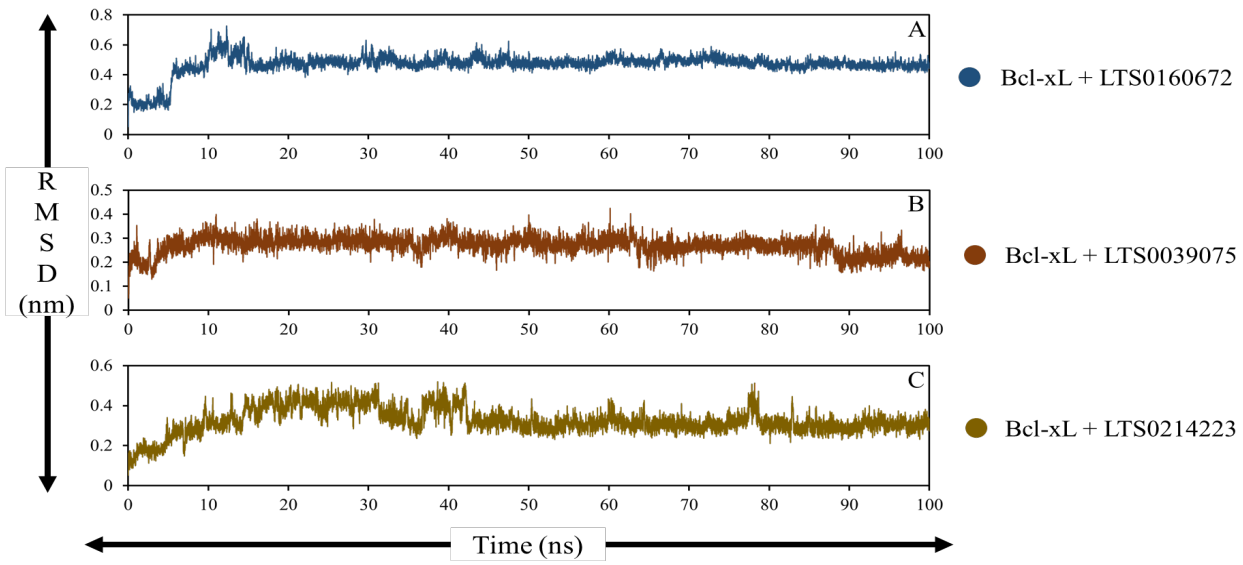

Figure 4. Root-Mean-Square Deviation of Ligand Fit on Bcl-xL Protein in MD Simulations. (A. RMSD of compound LTS0160672 (blue color). B. RMSD of compound LTS0160672 (organge color). C. RMSD of compound LTS0214223 (brown color))

(Table 4). Therefore, *A. paniculata* compounds should be used at the recommended dosages to ensure safety.

We conducted an in silico evaluation of the anticancer activity of LTS0160672, LTS0039075, and LTS0214223. The results indicate that LTS0160672 exhibits anticarcinogenic, antineoplastic, and antimetastatic activity, with Pa > 0.5 (Table 5). This compound also demonstrates potential as an apoptosis inducer, as it is predicted to be an apoptosis agonist with Pa > 0.5. Meanwhile, the two andrographidine derived compounds, LTS0039075 and LTS0214223, exhibit most of the key anticancer properties assessed in Table 5 with high confidence values (Pa > 0.5). These findings suggest that andrographidine compounds identified through in silico prediction possess strong anticancer potential. Therefore, LTS0160672, LTS0039075, and LTS0214223 were further evaluated for their ability to stably bind to the Bcl-xL protein.

Molecular dynamics simulation

The MD simulations of the three systems corresponding to the binding of LTS0160672, LTS0039075, and LTS0214223 with the Bcl-xL protein were conducted for 100 ns to evaluate the stability of protein-ligand interactions.

Table 4. Toxicity Prediction of Top Hits

	LTS0160672	LTS0039075	LTS0214223
Hepatotoxicity	Inactive	Inactive	Inactive
(Probability)	(0.92)	(0.82)	(0.82)
Cardiotoxicity	Active	Active	Active
(Probability)	(0.79)	(0.92)	(0.92)
Carcinogenicity	Inactive	Inactive	Inactive
(Probability)	(0.71)	(0.93)	(0.93)
Mutagenicity	Inactive	Inactive	Inactive
(Probability)	(0.91)	(0.78)	(0.78)
Cytotoxicity	Active	Active	Active
(Probability)	(0.74)	(0.58)	(0.58)
AMES toxicity	No	No	No
hERG I inhibitor	No	No	No
hERG II inhibitor	No	Yes	Yes
Skin Sensitisation	No	No	No
Predicted Toxicity Class	2	5	5
Predicted LD50	9mg/kg	5000mg/kg	5000mg/kg
Oral Rat Acute Toxicity (LD50)	2.643 mol/kg	2.623 mol/kg	2.807 mol/kg
Tetrahymena pyriformis toxicity	0.285 Log (µg/L)	0.285 Log (µg/L)	0.285 Log (µg/L)

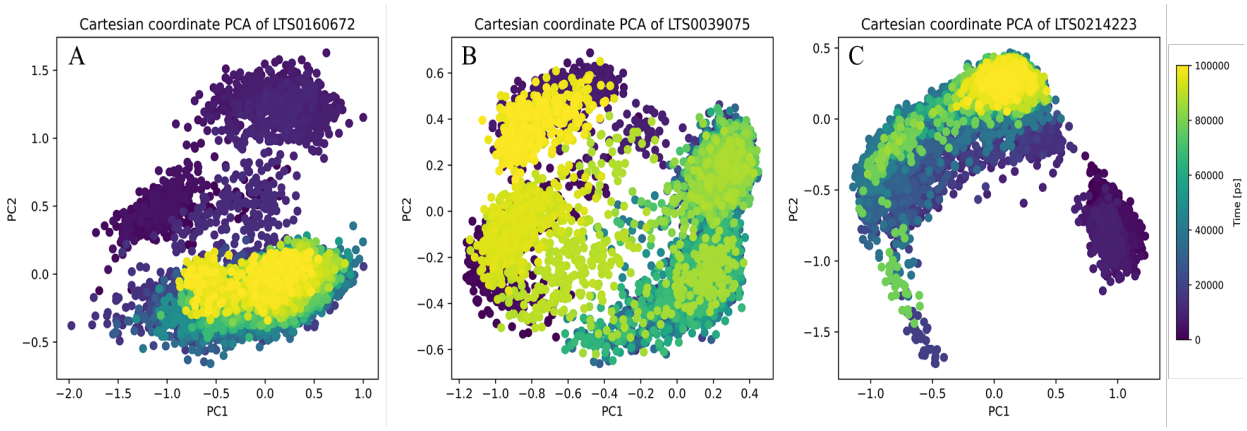

Figure 5. Cartesian Coordianate Principal Component Analysis of each Compound in 100 ns Simulation.

Table 5. Anticancer Activities Prediction of Top Hits.

	LTS0160672	LTS0039075	LTS0214223
	Pa		
TP53 enhancer	0.311	0.915	0.895
Anticarcinogenic	0.672	0.952	0.927
Apoptosis agonist	0.549	0.830	0.800
Antineoplastic	0.890	0.864	0.839
Antimetastatic	0.552	0.433	0.458
Cytostatic	0.264	0.869	0.832
Antimutagenic	-	0.767	0.652
Antioxidant	0.323	0.814	0.773
Myc inhibitor	0.475	0.508	0.520

Table 6. Total Binding Free Energy and Components of each Compound and Its Components (Kcal/mol).

	LTS0160672	LTS0039075	LTS0214223
ΔG_{vdw}	-46.97 ± 4.91	-58.07 ± 3.58	-49.08 ± 4.51
$\Delta G_{Eletrostatic}$	-18.64 ± 9.83	-19.07 ± 5.10	-25.25 ± 12.12
ΔG_{Gb}	35.52 ± 6.95	39.59 ± 3.99	42.25 ± 9.29
$\Delta G_{Non\text{-}polar}$	-6.57 ± 0.59	-7.20 ± 0.30	-6.51 ± 0.52
$\Delta G_{MM/GBSA}$	-36.66 ± 6.21	-44.74 ± 3.81	-38.60 ± 5.10

Analysis of the simulation trajectories revealed that the backbone of Bcl-xL protein maintained stable fluctuations throughout the 100 ns, with RMSD values for the Bcl-xL + LTS0160672, Bcl-xL + LTS0039075, and Bcl-xL + LTS0214223 systems recorded as 0.243 ± 0.023 nm, 0.211 ± 0.017 nm, and 0.212 ± 0.017 nm, respectively (Figure 3A). The radius of gyration analysis of Bcl-xL in these simulations indicated that the protein remained stably folded without significant structural perturbations,

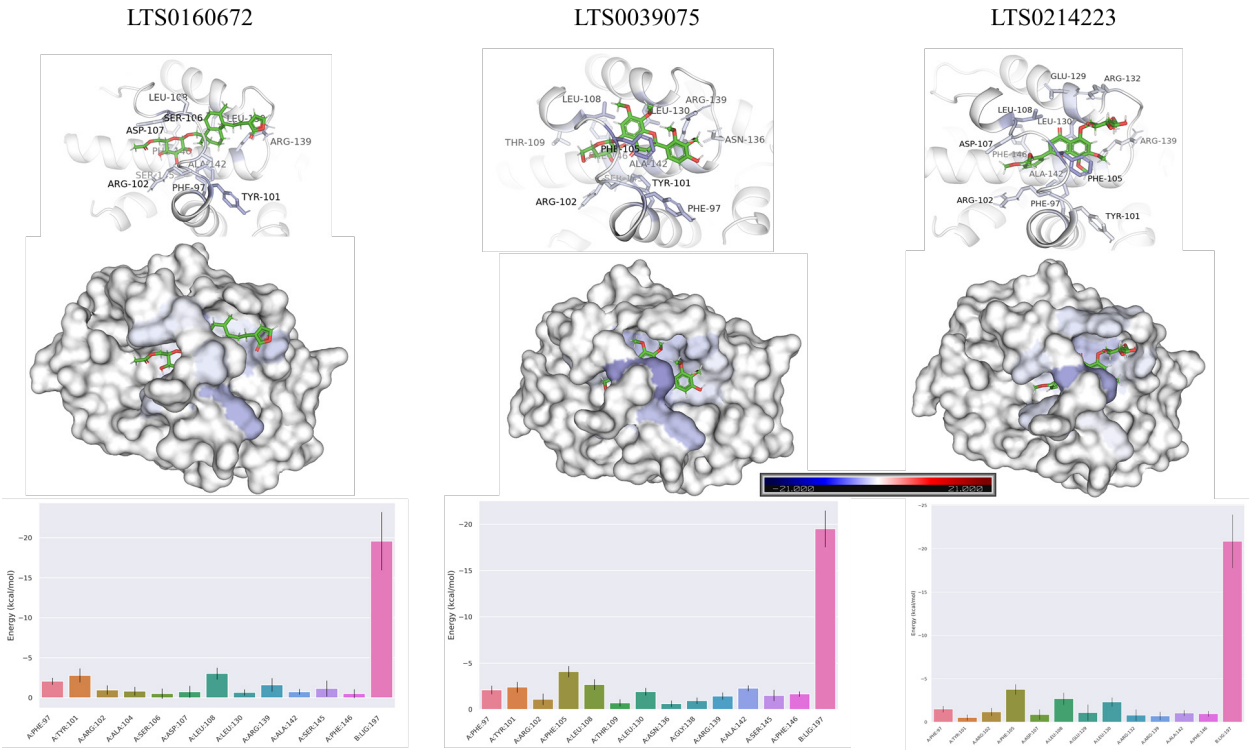

Figure 6. Amino Acid Interaction Energy Analysis of Each Compound with Bcl-xL in 100 ns Simulation.

with values of 1.456 ± 0.008 nm, 1.437 ± 0.007 nm, and 1.444 ± 0.007 nm for the Bcl-xL + LTS0160672, Bcl-xL + LTS0039075, and Bcl-xL + LTS0214223 systems, respectively (Figure 3B). Overall, the simulations reached equilibrium, and no drastic conformational changes in the target protein were observed upon ligand binding.

Next, it is crucial to evaluate the binding stability of the ligands within the Bcl-xL protein's hydrophobic groove. Therefore, RMSD analysis of the ligand fit on the protein was performed to assess the ligands' dynamic stability during their interaction with Bcl-xL. Analysis of the Bcl-xL + LTS0160672 system showed that the LTS0160672 molecule underwent minor repositioning from its predicted docking pose due to initial fluctuations during the early phase of the simulation (0 ns to 20 ns). However, it subsequently stabilized, maintaining an average RMSD value of 0.469 ± 0.069 nm (Figure 4A). In contrast, LTS0039075 and LTS0214223 exhibited stable binding within the hydrophobic groove of Bcl-xL throughout the 100 ns simulation, with RMSD values of 0.269 ± 0.037 nm (Figure 4B) and 0.325 ± 0.065 nm (Figure 4C), respectively.

PCA was conducted to assess the structural variations of the ligands during their interaction with Bcl-xL and their convergence behavior. Our analysis revealed that LTS0160672 underwent multiple structural changes between 0 ns and 20 ns (Figure 5A). However, from 20 ns to 100 ns, it exhibited positively correlated motion and structural convergence, indicating that it had stabilized (Figure 5A). The simulation trajectory of LTS0039075 displayed an undefined orientation, as no clear directionality was observed along either PC1 or PC2 (Figure 5B). Toward the end of the simulation, the collected structures tended to resemble the initial conformation, suggesting that the structural deviations throughout the simulation were minimal (Figure 5B). Meanwhile, LTS0214223 experienced initial structural rearrangements but later exhibited positively correlated motion in both PC1 and PC2, indicating structural convergence and overall ligand stability (Figure 5C). Thus, through RMSD and PCA analyses over the 100 ns simulation, we observed that the three compounds, LTS0160672, LTS0039075, and LTS0214223, demonstrated the ability to form stable chemical interactions and maintain strong structural correlations within the hydrophobic groove of the Bcl-xL protein (Figures 4 and Figures 5).

Binding free energy and decomposite analysis

The binding affinity of the ligands to the target protein is reflected by the binding free energy (BFE). Therefore, we computed this value using the MM/GBSA approach throughout a 100 ns simulation. Our analysis indicated that the BFE values remained stable throughout the simulation for all three compounds, with mean values of -36.66 ± 6.21 kcal/mol, -44.74 ± 3.81 kcal/mol, and -38.60 ± 5.10 kcal/mol for LTS0160672, LTS0039075, and LTS0214223, respectively (Table 6). Among the contributing forces, van der Waals and electrostatic interactions played a predominant role in stabilizing the ligand-protein interactions (Table 6). Further analysis of amino acid residues forming stable interactions with the studied compounds identified key residues within the hydrophobic groove of Bcl-xL, specifically 97PHE, 101TYR, 102ARG, 105PHE, 108LEU, 130LEU, 139ARG, 142ALA, and 146PHE, which maintained negative and stable binding energies with the ligands (Figure 6). Consequently, our findings suggest that LTS0160672, LTS0039075, and LTS0214223 effectively interact with critical residues within the active site of Bcl-xL, potentially inhibiting its interaction with pro-apoptotic proteins and thereby interfering with its anti-apoptotic function.

Discussion

Cancer is one of the most severe diseases claiming millions of lives each year. Despite advancements in modern therapeutic strategies, drug resistance and severe side effects remain significant challenges, particularly for patients with compromised health. Therefore, the incorporation of plant-derived natural extracts presents a promising alternative, offering greater accessibility and tolerability for a broader range of patients. Medicinal plants have long been regarded as a rich and diverse source of novel therapeutic agents, with an extensive repertoire of bioactive compounds exhibiting anticancer properties [49]. As a result, drug discovery and research organizations are increasingly focusing on computational and analytical approaches to develop natural compound libraries in the hope of identifying promising candidates for specific diseases [50, 51]. Notably, a study conducted by the National Cancer Institute (NCI) screened more than 150,000 compounds derived from various natural sources, including animals, plants, and microorganisms. This large-scale screening effort targeted all key members of the anti-apoptotic protein family, including Bcl-2, Bcl-W, Bcl-xL, Bcl-B, Mcl-1, and Bfl-1, in search of potential inhibitors [52].

A. paniculate is well known for its diterpenoid compound, andrographolide, which is characterized by an extremely bitter taste and exhibits significant anticancer properties [53, 54]. Numerous studies have reported the anticancer activity of andrographolide from *A. paniculate*, demonstrating its ability to inhibit the cell cycle, induce apoptosis, and regulate lipid-dependent cancer pathways [55-58]. In this study, we have, for the first time, identified flavonoid compounds from *A. paniculate* that exhibit strong and highly stable binding within the hydrophobic pocket of the Bcl-xL protein. Flavonoid compounds are known to inhibit cell proliferation and promote apoptosis via mitochondrial and endoplasmic reticulum pathways [59-61]. Some flavonoids have also been reported to reduce the synthesis of Bcl-2 and Bcl-xL proteins [59]. By extracting data from the LOTUS and OSADHI databases [62], we identified some andrographidine compounds are flavonoids (Figure 2), which are characteristic constituents of the Andrographis genus. This highlights the valuable pharmacological properties of this plant family. Through in silico predictions, we have demonstrated that two of the andrographidine compounds (LTS0039075, and LTS0214223) in this study not only exhibit anticancer activity but also form stable interactions with the active

site of the Bcl-xL protein. Similarly, we have identified a novel diterpenoid, LTS0160672, with potential for Bcl-xL inhibition and significant anticancer properties. This suggests that these compounds may serve as promising candidates for apoptosis-targeted cancer therapy.

Despite its limitations, our study significantly contributes to the research on Bcl-xL inhibitors. A notable finding of our research is the identification of natural compounds andrographidine which belong to *A. paniculate* as promising candidates for cancer treatment—beyond the well-known andrographolide. Although MD simulations can only partially capture the complex biological characteristics of Bcl-xL protein and its ligands, our study demonstrates that the investigated compounds exhibit strong binding affinity and possess favorable pharmacokinetic properties for potential oral drug development. An extended in silico study to evaluate these compounds against other anti-apoptotic targets would be an intriguing research direction that could significantly contribute to the advancement of targeted cancer therapies. Further in vitro, in vivo and eventual clinical investigations will be necessary to fully assess their therapeutic potential.

In conclusion, *A. paniculate* has attracted significant interest from researchers due to the potent anticancer properties of Andrographolide. In this study, we collected compounds extracted from *A. paniculate* available in the LOTUS database and identified andrographidine derivatives-LTS0039075, LTS0214223, and LTS0160672-belonging to the diterpenoid class, which exhibit strong and stable binding within the hydrophobic pocket of Bcl-xL. In silico pharmacokinetic and anticancer activity analyses indicate that all three compounds possess favorable properties as potential anticancer agents. They comply with Lipinski's rule of five, suggesting their suitability for oral drug development. However, to translate the findings of this study into clinical trials and drug development, further in-depth experimental investigations are required.

Author Contribution Statement

The corresponding author and each member of the writing team actively contributed to the research, data processing, discussion and preparation of this paper collectively and are responsible for its contents.

Acknowledgements

This research received no specific grant from any funding agency in the public, commercial, or non-profit sectors.

Conflict of Interests

The authors declare that there are no conflicts of interest related to this article.

Data Availability

Data presented in this study will be available on a fair request to the corresponding author.

References

1. Bray F, Laversanne M, Sung H, Ferlay J, Siegel RL, Soerjomataram I, et al. Global cancer statistics 2022: Globocan estimates of incidence and mortality worldwide for 36 cancers in 185 countries. CA Cancer J Clin. 2024;74(3):229-63. https://doi.org/10.3322/caac.21834.
2. Zhang CL, Huang T, Wu BL, He WX, Liu D. Stem cells in cancer therapy: Opportunities and challenges. Oncotarget. 2017;8(43):75756-66. https://doi.org/ 10.18632/oncotarget.20798.
3. Prieto-Vila M, Takahashi RU, Usuba W, Kohama I, Ochiya T. Drug resistance driven by cancer stem cells and their niche. Int J Mol Sci. 2017;18(12):2574. https://doi.org/ 10.3390/ijms18122574.
4. Housman G, Byler S, Heerboth S, Lapinska K, Longacre M, Snyder N, et al. Drug resistance in cancer: An overview. Cancers. 2014;6(3):1769-92. https://doi.org/10.3390/cancers6031769.
5. Alhmoud JF, Woolley JF, Al Moustafa AE, Malki MI. DNA damage/repair management in cancers. Cancers. 2020;12(4):1050. https://doi.org/10.3390/cancers12041050.
6. Kastan MB, Bartek J. Cell-cycle checkpoints and cancer. Nature. 2004;432(7015):316-23. https://doi.org/10.1038/nature03097.
7. Jacobson MD, Weil M, Raff MC. Programmed cell death in animal development. Cell. 1997;88(3):347-54. https://doi.org/10.1016/s0092-8674(00)81873-5.
8. Carneiro BA, El-Deiry WS. Targeting apoptosis in cancer therapy. Nature reviews Clinical oncology. 2020;17(7):395-417. https://doi.org/10.1038/s41571-020-0341-y.
9. Tsujimoto Y, Finger LR, Yunis J, Nowell PC, Croce CM. Cloning of the chromosome breakpoint of neoplastic b cells with the t(14;18) chromosome translocation. Science (New York, NY). 1984;226(4678):1097-9. https://doi.org/10.1126/science.6093263.
10. Reed JC. Bcl-2 family proteins: Regulators of apoptosis and chemoresistance in hematologic malignancies. Semin Hematol. 1997;34(4 Suppl 5):9-19.
11. Chao DT, Korsmeyer SJ. Bcl-2 family: Regulators of cell death. Annu Rev Immunol. 1998;16:395-419. https://doi.org/10.1146/annurev.immunol.16.1.395.
12. Martinou JC, Youle RJ. Mitochondria in apoptosis: Bcl-2 family members and mitochondrial dynamics. Developmental cell. 2011;21(1):92-101. https://doi.org/10.1016/j.devcel.2011.06.017.
13. Youle RJ, Strasser A. The bcl-2 protein family: Opposing activities that mediate cell death. Nat Rev Mol Cell Biol. 2008;9(1):47-59. https://doi.org/10.1038/nrm2308.
14. Borrás C, Mas-Bargues C, Román-Domínguez A, Sanz-Ros J, Gimeno-Mallench L, Inglés M, et al. Bcl-xl, a mitochondrial protein involved in successful aging: From c. Elegans to human centenarians. Int J Mol Sci. 2020;21(2). https://doi.org/10.3390/ijms21020418.
15. Zhang L, Li J, Tian D, Sun L, Wang X, Tian M. Theranostic combinatorial drug-loaded coated cubosomes for enhanced targeting and efficacy against cancer cells. Cell Death Dis. 2020;11(1):1. https://doi.org/10.1038/s41419-019-2182-0.
16. Li M, Wang D, He J, Chen L, Li H. Bcl-xl: A multifunctional anti-apoptotic protein. Pharmacol Res. 2020;151:104547. https://doi.org/10.1016/j.phrs.2019.104547.
17. Oltersdorf T, Elmore SW, Shoemaker AR, Armstrong RC, Augeri DJ, Belli BA, et al. An inhibitor of bcl-2 family proteins induces regression of solid tumours. Nature. 2005;435(7042):677-81. https://doi.org/10.1038/nature03579.
18. Hossain SL, Mathews M, Bhyranalyar Nagarajappa

VS, Kumar BK, Veerappa Yelamaggad CV, C RS. Antiproliferative, apoptosis-inducing activity and molecular docking studies of sydnones compounds. J Cancer Res Ther. 2022;18(3):681–90. https://doi.org/10.4103/jcrt.JCRT_1614_20.
19. Rasooli I, editor. Phytochemicals: Bioactivities and Impact on Health. 1st ed. BoD–Books on Demand; 2011 Dec 22.
20. Roy A, Attre T, Bharadvaja N, Tiezzi A, Karpiński T. New aspects in medicinal plants and pharmacognosy. 1st ed. Poznań, Poland: JBBooks; 2017.
21. Kala CP, Dhyani PP, Sajwan BS. Developing the medicinal plants sector in northern india: Challenges and opportunities. J Ethnobiol Ethnomed. 2006;2:32. https://doi.org/10.1186/1746-4269-2-32.
22. Mehta V, Chander H, Munshi A. Mechanisms of anti-tumor activity of withania somnifera (ashwagandha). Nutrit Cancer. 2021;73(6):914-26. https://doi.org/10.1080/01635581.2020.1778746.
23. Okhuarobo A, Falodun JE, Erharuyi O, Imieje V, Falodun A, Langer P. Harnessing the medicinal properties of andrographis paniculata for diseases and beyond: A review of its phytochemistry and pharmacology. Asian Pac J Trop Dis. 2014;4(3):213–22. https://doi.org/10.1016/S2222-1808(14)60509-0.
24. Jiaqi H, Yunfei D, Daniel T. Andrographis wallich ex nees in wallich. Flora of China. 2011;19:473-74.
25. Hossain S, Urbi Z, Karuniawati H, Mohiuddin RB, Moh Qrimida A, Allzrag AMM, et al. *Andrographis paniculata* (burm. F.) wall. Ex nees: An updated review of phytochemistry, antimicrobial pharmacology, and clinical safety and efficacy. Life. 2021;11(4):348. https://doi.org/10.3390/life11040348.
26. World Health Organization. WHO monographs on selected medicinal plants.2nd ed. Italy: Ravello-Salerno; 1999.
27. Mishra SK, Sangwan NS, Sangwan RS. *Andrographis paniculata* (kalmegh): A review. Phcog Rev. 2007;1(2):283-98.
28. Khare CP. Indian medicinal plants: an illustrated dictionary. 1st ed. New York: Springer New York, NY; 2007.
29. Wang L, Doherty GA, Judd AS, Tao Z-F, Hansen TM, Frey RR, et al. Discovery of a-1331852, a first-in-class, potent, and orally-bioavailable bcl-xl inhibitor. ACS Med Chem Lett. 2020;11(10):1829-36. https://doi.org/10.1021/acsmedchemlett.9b00568.
30. Morris GM, Huey R, Lindstrom W, Sanner MF, Belew RK, Goodsell DS, et al. Autodock4 and autodocktools4: Automated docking with selective receptor flexibility. J Comput Chem. 2009;30(16):2785-91. https://doi.org/10.1002/jcc.21256.
31. Rutz A, Sorokina M, Galgonek J, Mietchen D, Willighagen E, Gaudry A, et al. The lotus initiative for open knowledge management in natural products research. eLife. 2022;11:e70780. https://doi.org/10.7554/eLife.70780.
32. O'Boyle NM, Banck M, James CA, Morley C, Vandermeersch T, Hutchison GR. Open babel: An open chemical toolbox. J Cheminform. 2011;3(1):33. https://doi.org/10.1186/1758-2946-3-33.
33. Santos-Martins D, Solis-Vasquez L, Tillack AF, Sanner MF, Koch A, Forli S. Accelerating autodock4 with gpus and gradient-based local search. J Chem Theory Comput. 2021;17(2):1060-73. https://doi.org/10.1021/acs.jctc.0c01006.
34. Adasme MF, Linnemann KL, Bolz SN, Kaiser F, Salentin S, Haupt V J, et al. Plip 2021: Expanding the scope of the protein–ligand interaction profiler to DNA and rna. Nucleic Acids Res. 2021;49(W1):W530-W4. https://doi.org/10.1093/nar/gkab294.
35. Daina A, Michielin O, Zoete V. Swissadme: A free web tool to evaluate pharmacokinetics, drug-likeness and medicinal chemistry friendliness of small molecules. Sci Rep. 2017;7(1):42717. https://doi.org/10.1038/srep42717.
36. Banerjee P, Kemmler E, Dunkel M, Preissner R. Protox 3.0: A webserver for the prediction of toxicity of chemicals. Nucleic Acids Res. 2024;52(W1):W513-W20. https://doi.org/10.1093/nar/gkae303.
37. Pires DE, Blundell TL, Ascher DB. Pkcsm: Predicting small-molecule pharmacokinetic and toxicity properties using graph-based signatures. J Med Chem. 2015;58(9):4066-72. https://doi.org/10.1021/acs.jmedchem.5b00104.
38. Filimonov DA, Lagunin AA, Gloriozova TA, Rudik AV, Druzhilovskii DS, Pogodin PV, et al. Prediction of the biological activity spectra of organic compounds using the pass online web resource. Chem Heterocycl Comp. 2014;50(3):444-57. https://doi.org/10.1007/s10593-014-1496-1.
39. Abraham MJ, Murtola T, Schulz R, Páll S, Smith JC, Hess B, et al. Gromacs: High performance molecular simulations through multi-level parallelism from laptops to supercomputers. SoftwareX. 2015;1:19-25. https://doi.org/10.1016/j.softx.2015.06.001.
40. Zoete V, Cuendet MA, Grosdidier A, Michielin O. Swissparam: A fast force field generation tool for small organic molecules. J comput chem. 2011;32(11):2359-68. https://doi.org/10.1002/jcc.21816.
41. Huang J, MacKerell AD, Jr. Charmm36 all-atom additive protein force field: Validation based on comparison to nmr data. J comput chem. 2013;34(25):2135-45. https://doi.org/10.1002/jcc.23354.
42. McGibbon RT, Beauchamp KA, Harrigan MP, Klein C, Swails JM, Hernández CX, et al. Mdtraj: A modern open library for the analysis of molecular dynamics trajectories. Biophys J. 2015;109(8):1528-32. https://doi.org/10.1016/j.bpj.2015.08.015.
43. Valdés-Tresanco MS, Valdés-Tresanco ME, Valiente PA, Moreno E. Gmx_mmpbsa: A new tool to perform end-state free energy calculations with gromacs. J Chem Theory Comput. 2021;17(10):6281-91. https://doi.org/10.1021/acs.jctc.1c00645.
44. Wang H, Guo M, Wei H, Chen Y. Structural basis of the specificity and interaction mechanism of bmf binding to pro-survival bcl-2 family proteins. Comput Struct Biotechnol J. 2023;21:3760-7. https://doi.org/10.1016/j.csbj.2023.07.017.
45. Cáceres DD, Hancke JL, Burgos RA, Sandberg F, Wikman GK. Use of visual analogue scale measurements (vas) to asses the effectiveness of standardized andrographis paniculata extract sha-10 in reducing the symptoms of common cold. A randomized double blind-placebo study. Phytomedicine. 1999;6(4):217-23. https://doi.org/10.1016/S0944-7113(99)80012-9.
46. Melchior J, Spasov AA, Ostrovskij OV, Bulanov AE, Wikman G. Double-blind, placebo-controlled pilot and phase iii study of activity of standardized andrographis paniculata herba nees extract fixed combination (kan jang) in the treatment of uncomplicated upper-respiratory tract infection. Phytomedicine. 2000;7(5):341-50. https://doi.org/10.1016/S0944-7113(00)80053-7.
47. Amaryan G, Astvatsatryan V, Gabrielyan E, Panossian A, Panosyan V, Wikman G. Double-blind, placebo-controlled, randomized, pilot clinical trial of immunoguard--a standardized fixed combination of andrographis paniculata nees, with eleutherococcus senticosus maxim, schizandra chinensis bail. And glycyrrhiza glabra l. Extracts in patients with familial mediterranean fever. Phytomedicine : international journal of phytotherapy

and phytopharmacology. 2003;10(4):271-85. https://doi.org/10.1078/094471103322004767.
48. Mkrtchyan A, Panosyan V, Panossian A, Wikman G, Wagner H. A phase i clinical study of andrographis paniculata fixed combination kan jang versus ginseng and valerian on the semen quality of healthy male subjects. Phytomedicine. 2005;12(6-7):403-9. https://doi.org/10.1016/j.phymed.2004.10.004.
49. Dakkak BE, Taneera J, El-Huneidi W, Abu-Gharbieh E, Hamoudi R, Semreen MH, et al. Unlocking the therapeutic potential of bcl-2 associated protein family: Exploring bcl-2 inhibitors in cancer therapy. Biomol ther. 2024;32(3):267-80. https://doi.org/10.4062/biomolther.2023.149.
50. Thornburg CC, Britt JR, Evans JR, Akee RK, Whitt JA, Trinh SK, et al. Nci program for natural product discovery: A publicly-accessible library of natural product fractions for high-throughput screening. ACS Chem Biol. 2018;13(9):2484-97. https://doi.org/10.1021/acschembio.8b00389.
51. Eldesouki S, Qadri R, Abu Helwa R, Barqawi H, Bustanji Y, Abu-Gharbieh E, et al. Recent updates on the functional impact of kahweol and cafestol on cancer. Molecules (Basel, Switzerland). 2022;27(21):7332. https://doi.org/10.3390/molecules27217332.
52. Hassig CA, Zeng FY, Kung P, Kiankarimi M, Kim S, Diaz PW, et al. Ultra-high-throughput screening of natural product extracts to identify proapoptotic inhibitors of bcl-2 family proteins. J Biomol Screen. 2014;19(8):1201-11. https://doi.org/10.1177/1087057114536227.
53. Lee YC, Lin HH, Hsu CH, Wang CJ, Chiang TA, Chen JH. Inhibitory effects of andrographolide on migration and invasion in human non-small cell lung cancer a549 cells via down-regulation of pi3k/akt signaling pathway. Eur j pharmacol. 2010;632(1-3):23-32. https://doi.org/10.1016/j.ejphar.2010.01.009.
54. Islam MT, Ali ES, Uddin SJ, Islam MA, Shaw S, Khan IN, et al. Andrographolide, a diterpene lactone from andrographis paniculata and its therapeutic promises in cancer. Cancer lett. 2018;420:129-45. https://doi.org/10.1016/j.canlet.2018.01.074.
55. Yang L, Wu D, Luo K, Wu S, Wu P. Andrographolide enhances 5-fluorouracil-induced apoptosis via caspase-8-dependent mitochondrial pathway involving p53 participation in hepatocellular carcinoma (smmc-7721) cells. Cancer letters. 2009;276(2):180-8. https://doi.org/ 10.1016/j.canlet.2008.11.015.
56. Tohkayomatee R, Reabroi S, Tungmunnithum D, Parichatikanond W, Pinthong D. Andrographolide exhibits anticancer activity against breast cancer cells (mcf-7 and mda-mb-231 cells) through suppressing cell proliferation and inducing cell apoptosis via inactivation of er-α receptor and pi3k/akt/mtor signaling. Molecules (Basel, Switzerland). 2022;27(11):3544. https://doi.org/10.3390/molecules27113544.
57. Naomi R, Bahari H, Ong ZY, Keong YY, Embong H, Rajandram R, et al. Mechanisms of natural extracts of andrographis paniculata that target lipid-dependent cancer pathways: A view from the signaling pathway. Int J Mol Sci. 2022;23(11):5972. https://doi.org/10.3390/ijms23115972.
58. Shi MD, Lin HH, Lee YC, Chao JK, Lin RA, Chen JH. Inhibition of cell-cycle progression in human colorectal carcinoma lovo cells by andrographolide. Chemico-biological interactions. 2008;174(3):201-10. https://doi.org/10.1016/j.cbi.2008.06.006.
59. Bahadar N, Bahadar S, Sajid A, Wahid M, Ali G, Alghamdi A, et al. Epigallocatechin gallate and curcumin inhibit bcl-2: A pharmacophore and docking based approach against cancer. Breast Cancer Res. 2024;26(1):114. https://doi.org/10.1186/s13058-024-01868-9.
60. Hu D, Zhang L, Qin B, Wang N, Li X, Shi W. Association between urinary lead and female breast cancer: A population-based cross-sectional study. Discovery medicine. 2023;35(179):1177-89. https://doi.org/10.24976/Discov.Med.202335179.114.
61. Li M, Wei J, Xue C, Zhou X, Chen S, Zheng L, et al. Dissecting the roles and clinical potential of yy1 in the tumor microenvironment. Frontiers in oncology. 2023;13:1122110. https://doi.org/10.3389/fonc.2023.1122110.
62. Kiewhuo K, Gogoi D, Mahanta HJ, Rawal RK, Das D, S V, et al. Osadhi – an online structural and analytics based database for herbs of india. Comput Biol Chem. 2023;102:107799. https://doi.org/10.1016/j.compbiolchem.2022.107799.